DEPENDENCE OF UPSTREAM MOVING PRESSURE WAVES ON THE MACH NUMBER AND THE IMPACT OF TRAILING EDGE SERRATIONS

J. M. Nies and H. Olivier, Shock Wave Laboratory, RWTH Aachen University

Abstract

The dependence of upstream moving pressure waves on the free stream and the local Mach number is investigated on the supercritical BAC 3-11 airfoil in transonic flow. The high-instationary behavior of the waves is analyzed in detail from the very weak pressure waves at a subsonic Mach number of $M_\infty = 0.63$ to a stationary shock at a transonic Mach number $M_\infty = 0.79$. Due to the increasing free stream Mach number the pressure waves gain strength which is accompanied by their steepening and fusion, leading to the formation of instationary shock waves. A further increase of the free stream Mach number finally results in the formation of a recompression shock at an approximate Mach number of $M_\infty = 0.78$.
In a second step a serrated splitter plate is applied to the trailing edge in order to disturb the vortex/trailing edge interaction which is one of the development mechanism of the pressure waves. The influence of the serrated splitter plate is examined with the focus on the change in wave amplitude and wave behavior.

SYMBOLS AND ABBREVIATIONS

a	=	speed of sound, m/s
c	=	chord length, mm
f	=	frequency, Hz
$2h$	=	saw tooth length, mm
M	=	Mach number
p	=	pressure, bar
Re	=	Reynolds number
Sr	=	Strouhal number, $Sr_c = \frac{f \cdot c}{u_\infty}$
t	=	time, s
T	=	temperature, K
u, U	=	velocity, m/s
δ	=	boundary layer thickness, mm
κ	=	acoustic wavenumber, $\kappa = \frac{\omega}{a}$, rad/m
λ	=	serration width, wave length, mm
φ	=	phase angle, geometrical flank angle, 1°
ρ	=	density, kg/m^3
σ	=	standard deviation

Subscript

∞	=	free stream
l	=	local
c	=	chord

1 INTRODUCTION

Pressure waves of transonic airfoil flow, also called Kutta, acoustic or compression waves, are mostly known from buffet [1], transonic flutter [2] or the flow around oscillating airfoils and flaps [3].
Lee [1], for example, focuses on the buffet mechanism. He refers to the pressure waves as part of his model of self-sustained shock oscillation of the buffet mechanism. In his model, the shock movement induces pressure waves propagating within the separated flow downstream, which then interact with the trailing edge to generate upstream moving pressure waves. These upstream moving pressure waves therefore interact with the shock and sustain its oscillation.
Voss [2] concentrated on the propagation of pressure waves in transonic flows with the aim of simulating the flutter process numerically by the help of the linearized potential equations and the acoustic theory. Due to the use of the linearized potential equations, it is not possible to give quantitative information about the wave amplitude and the formation of a shock. That is why this paper will focus on the experimentally obtained pressure amplitude of the waves.
Tijdeman [3] also examined the behavior of the pressure waves, prevalent in experiments, but on oscillating airfoils and on an airfoil with an oscillating trailing edge flap. In his work three different types of wave movements have been defined, Type A a sinusoidal motion of the shock, Type B a shock that vanishes during a part of its almost sinusoidal cycle and Type C, where weak compression waves coalesce to form a shock, which moves upstream and surpasses the leading edge into the free stream.

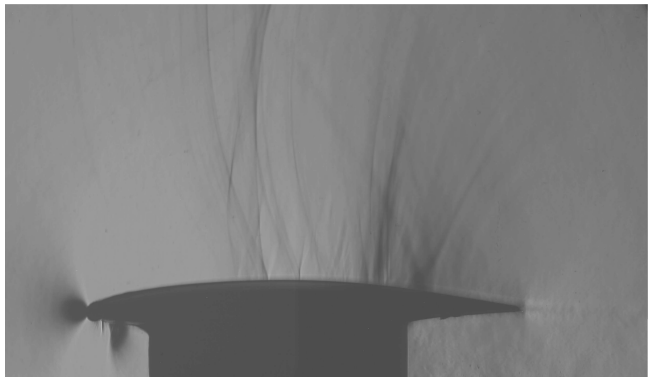

Fig. 1: Schlieren image of BAC 3-11 at $M_\infty = 0.76$ and $Re_c = 1 \cdot 10^6$

However, it was found that the waves can also develop naturally, far below the buffet onset and without sep-

aration by a number of different mechanism. Figure 1 shows these natural pressure waves on the BAC 3-11 at a Mach number of 0.75 and a chord Reynolds number of $1 \cdot 10^6$.
Some of the development mechanism of the waves can be classified. Firstly, if the Mach number is high enough, local supersonic regions, which are induced by vortices near the airfoil surface, can induce pressure waves. Secondly, the interaction between vortices and the recompression shock on the airfoil can provoke pressure waves. Thirdly, they can develop by the interaction of vortices with the trailing edge, and fourthly, the wake oscillations. These four classified mechanism have been observed by Hermes [4] and Klioutchnikov [5] in their numerical simulations of the transonic flow around a two-dimensional BAC 3-11 airfoil.
Further, it is determined that the pressure waves can merge and steepen up to form weak shock waves on their way upstream along the suction side of the airfoil. This was observed on the two-dimensional BAC 3-11 airfoil in numerical simulations done by Hermes [4, 6] as well as in experiments in the Transonic Shock Tube (STK) by Al Shabu [7]. These processes will be described in more detail in the first part of the paper.
Recently, Ballmann [8] observed the pressure waves also on a wing, based on the same BAC 3-11 shape, during experiments in the European Transonic Wind Tunnel at quasi-stationary flows at Mach numbers between 0.7 and 0.8 and a Reynolds number of $23 \cdot 10^6$. The reason why these waves behave in such a complex way lies in the complexity of the flow around the supercritical airfoil itself. The flow is strongly influenced by the airfoil shape and therefore also by its local pressure gradient, which affects the local flow velocity. It was found that these parameters determine the wave behavior, accordingly the propagation of the waves, as well as their steepening process. This has already been mentioned by Spee [9] in 1966 who observed the waves experimentally in schlieren pictures, comparing them with the solutions of the potential equations for compressible airflow found by Nieuwland [10].
Although upstream moving pressure waves on transonic airfoils appear to have various influences on the flow, only few studies have been published on this topic.
Thus, the first part of the paper will focus on the behavior of the pressure waves during their movement over the BAC 3-11 and analyze its dependence on the Mach number as well as the influence of the waves on the shock formation.
The second part of the paper will deal with the impact of a trailing edge serration on the wave amplitude and the wave behavior. The serration will influence the developing mechanism of the waves due to vortex/trailing edge interaction as well as the wake oscillation and therefore reduce the strength of the pressure waves.
Trailing edge serrations are mostly known from acoustics where they are used to reduce aerodynamic noise, for example at the take-off and landing of airplanes or on wind turbine blades. Usage of trailing edge serrations at a sharp trailing edge in transonic speeds is not know to the author. However, the pressure waves studied in this paper have the same origin as the acoustic wave in incompressible flow. The difference of the two wave kinds lies in their strength and the steepening effect due to the transonic speed. This is why the solutions of the differential equations change from linear in incompressible flow to non-linear in compressible flow.
An analytical theory of the noise reduction of a regular serrated trailing edge at low Mach numbers $M_\infty < 0.4$ has been formulated by Howe [11, 12]. He suggests an angle of less than 45° for the serration because he discovered that a significant amount of noise is produced by the interaction of vortices having a wave-number vector normal to the trailing edge. Therefore, the noise should be reduced if the angle between the vortices and the edge is decreased. A further noise reduction is gained by the reduction of the effective spanwise length of the trailing edge due to the serration.
Oerlemans et al. [13] examined the trailing edge noise reduction on wind turbine blades with a shape optimizations of the airfoil, a trailing edge serration and a combination of both. The length of the serration was about 20% of the local chord of the blade. The modifications showed a significant trailing edge noise reduction in the low frequency range as well as an increase in noise reduction with increasing wind speeds (6-10 m/s). The modifications were found to have no adverse effect on the aerodynamic performance.
Jones and Sandberg [14] conducted recently Direct Numerical Simulations (DNS) of the flow around straight and serrated splitter plates at a NACA-0012 airfoil at $M_\infty = 0.4$. A significant reduction of the amplitude of all frequencies above $Sr \approx 5$ have been found for the serrated trailing edge due to changes of the scattering process of the waves.
These successful applications of serrated trailing edges motivated their use also in compressible subsonic and transonic airfoil flows.

2 EXPERIMENTAL SETUP AND PROCEDURE

2.1 Shock Tube

The experiments have been conducted in a modified shock tube (STK) for the testing of transonic airfoils. The shock tube consists of five main parts, the high pressure part, followed by the double membrane chamber, linked to the low pressure part which is connected to the test section, concluding in a vessel. The rectangular test section holds cookie cutters to remove the shock tube boundary layer on the top, bottom and side walls of the test section. The performance covers

a free stream Mach number range of 0.6 to 1.2 and can reach Reynolds numbers up to $Re_c = 38 \cdot 10^6$ based on a chord length of 100 mm.
Mach and Reynolds number can be varied independently. By increasing the absolute pressure levels in the high pressure and low pressure section the Reynolds number rises. If the pressure ratio of the high pressure section to the low pressure section is increased also the Mach number increases.
After the high and low pressure tube are filled to the correct pressures, the membranes burst and the shock wave develops. The shock wave travels down the shock tube through the test section into the vessel inducing the quasi-stationary flow. The main disadvantage, which is typical for all impulse test facilities, is the relative short testing time of 4 - 10 ms. Nevertheless, the testing time is sufficient to establish a quasi-stationary flow and perform reliable measurements. To reduce the influence of the channel walls a comparably thin airfoil model with 8.8 mm thickness is used in a rectangular test section with a size of 280 x 200 mm. The free stream Mach number is deduced from Pitot and static pressure transducers, which are mounted in the upstream flow. A full description of the facility and its working principle can be found in Zechner [15].

2.2 Airfoil

The wind tunnel model is a BAC 3-11 airfoil of 8.8 mm thickness and a constant chord length of 80 mm. Eleven Kulite XCQ-080 pressure transducers are installed at the positions x/c = 0.11, 0.18, 0.24, 0.31, 0.37, 0.43, 0.49, 0.55, 0.61, 0.67 and 0.73. They are placed in a cavity which is connected to the flow by a short pressure hole with a diameter of 0.6 mm. The cutoff frequency of this arrangement is higher than 13 kHz. Each pressure signal is amplified by a factor of 100 and filtered with a hardware filter of 50 kHz by a MV 1000 amplifier. All sensors are sampled simultaneously with an NI 6133 measurement card at a sampling frequency of 10^6 Hz.
The airfoil is fixed with two support plates on the side walls of the tunnel so that only the flow above the airfoil is visible on schlieren images. Because of high mechanical loads it is not possible to fix the airfoil directly to the windows [15].
The measurement uncertainties of the flow parameters in the STK are given by Alshabu at al. [16] as following: pressure ±3 %, M = ±4.7 %, Re = ±5.8 %, and velocity ±4.5%. Due to the increasing boundary layer thickness inside the shock tube, there is a rise in Mach number of about 1.4 % during the measurment time. The Mach numbers quoted in this paper are corrected in order to take into account the blockage effect of the model and the model support system. The geometrical blockage effect leads to a Mach number increase of 5 %.

2.3 Visualization

A high-speed schlieren system is used for the flow visualization consisting of a typical Toepler-Z configuration. The pictures have been recorded with a Shimadzu HPV-1, which has a resolution of 312 x 260 pixels. Recording at a frame rate of 63 kfps, the full exposure time of 8 μs is needed.
Furthermore, single pictures have been made with a conventional Canon 5DS camera using the same schlieren system. Here, a nano-spark light-source replaces the continuous light source. The single pictures have a high resolution (12.8 MP) and an extreme short exposure time ($\leq$ 500 ns) hence providing very sharp and detailed views of the waves and the wake.

2.4 Data Processing

In order to derive a comparable physical quantity of the pressure waves the standard deviation of the pressure signals is calculated. Furthermore, the amplitude of specific frequencies is derived by a fast Fourier transformation (FFT).
To reduce initial disturbances and to derive a stationary flow, the measurement interval is placed 4 ms after the initial shock has passed the airfoil. The analysis is done at a time interval of $\Delta t = 4$ ms. Moreover, the values of the amplitude and the standard deviation are normalized by the static pressure of the free stream, making them independent of the Reynolds number for this type of facility.
The FFT is done by the standard Matlab routine.
The standard deviation σ of the pressure is calculated as following:

$$\sigma = \sqrt{\frac{1}{N-1}\sum_{n=1}^{N}(p-\bar{p})^2} \tag{1}$$

Moreover, the reduced frequency, respectively the Strouhal number, is calculated with the chord length as the characteristic length, the measured frequency and the free stream velocity.

$$Sr_c = \frac{f \cdot c}{u_\infty} \tag{2}$$

3 RESULTS

3.1 Wave Behavior

Upstream moving pressure waves with a highly complex propagation behavior are observed in the transonic flow around the supercritical BAC 3-11 airfoil. The waves are extremely sensible to Mach number changes. In the following, this propagation behavior will be explained within a Mach number range of 0.63

to 0.79 at a Reynolds number of $Re_c = 1 \cdot 10^6$ based on the chord length. Former experiments [7] showed no dependence of the waves on the Reynolds number in the range of $1 \cdot 10^6 < Re_c < 5 \cdot 10^6$, therefore no Reynolds number variation was conducted. All experiments have been performed at zero angle of attack.
The flow around the airfoil can be split in three characteristic velocity regimes. Firstly, the pure subsonic flow ($M_\infty < 0.72$) for which nowhere on the airfoil the speed of sound is reached. Secondly, the intermediate regime ($0.72 < M_\infty < 0.78$) with a region of supersonic speed on the suction side of the airfoil but without stationary shock. Thirdly, the transonic regime ($M_\infty > 0.78$) where the supersonic regime finishes with a stationary shock.
In all regimes upstream moving pressure waves can be observed with schlieren pictures and dynamic pressure measurements. The pressure amplitudes of the waves obtained by the FFT are shown in Figure 2 for a Mach number of 0.71. As can be seen, the characteristic frequencies of the waves are f = 1 kHz and 1.5 kHz, leading to Strouhal numbers of $Sr_c \approx 0.3$ and 0.45 ($Sr_c = f \cdot c/u_\infty$). The values for the two frequencies and the Strouhal numbers are consistent for the complete Mach number range. Therefore, this two frequencies will be focused in the following. In addition, the standard deviation will be given. It takes all pressure fluctuations into account so that a comparison of the standard deviation with the FFT will attest that both are adequate to measure the waves.

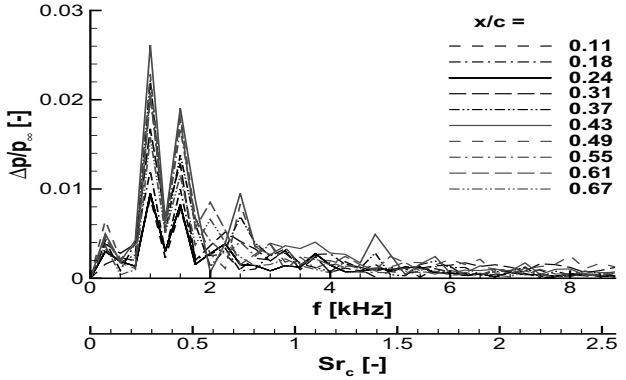

Fig. 2: FFT, no serration, $M_\infty = 0.71$ at x/c = 0.11 to 0.67

In Fig. 3 the normalized pressure amplitude for 1 kHz and 1.5 kHz as well as the standard deviation are plotted over the sensor position for the Mach number $M_\infty = 0.71$. The values for the two frequencies have been derived from the FFT whereas the standard deviation is calculated directly from the pressure signals for the same time interval. All three curves show the same shape. Typically, the normalized amplitude of the standard deviation has the highest values because it includes the pressure fluctuations of all frequencies including aerodynamic broadband noise as well as possible noise from the measurement system. The values of the 1 kHz frequency are very close to the one of the standard deviation whereas the amplitude of the 1.5 kHz is always significantly smaller. This is consistent for all examined Mach numbers.

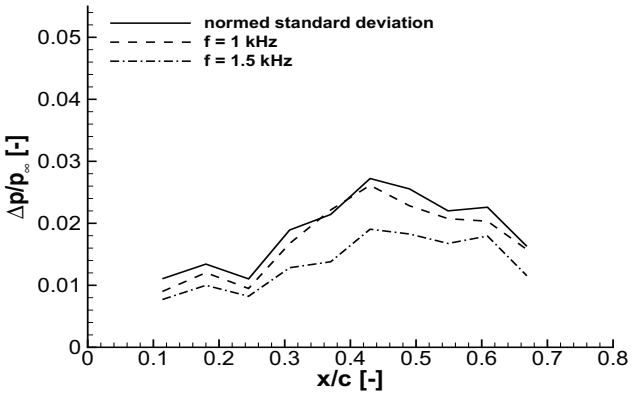

Fig. 3: Pressure amplitude over sensor position for f = 1 kHz, 1.5 kHz and normed standard deviation at $M_\infty = 0.71$

Since the 1 kHz frequency is more prominent than the 1.5 kHz one, the amplitude plots of the 1 kHz will be used to explain the phenomena of the wave propagation as a function of the free stream Mach number.
Figures 4, 5, 7 and 12 show the normalized pressure amplitude of the 1 kHz frequency over the sensor position for Mach numbers between 0.63 to 0.79.

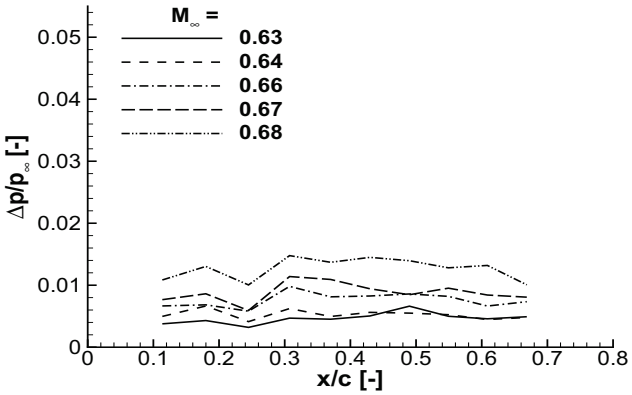

Fig. 4: Pressure amplitude for f = 1 kHz at $M_\infty = 0.63$ - 0.68

Fig. 4 shows the pressure amplitude over the sensor position for the pure subsonic flow at Mach numbers of 0.63 to 0.68. In this flow regime, the pressure waves move along the complete airfoil from the trailing edge to the leading edge with a rather constant amplitude. The pressure level with $\Delta p/p_\infty < 0.015$ is very low. The waves are also hardly detectable on the schlieren pictures and hence are not included in the paper.

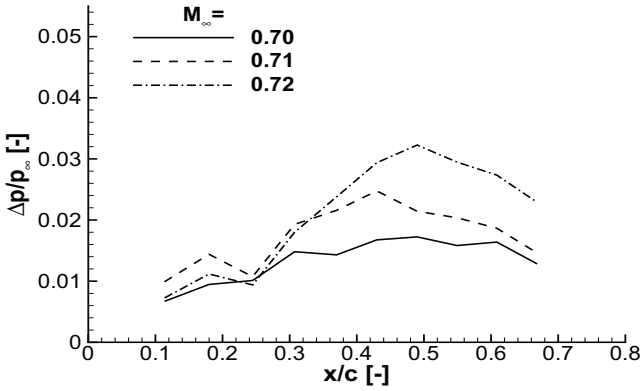

Fig. 5: Pressure amplitude for f = 1 kHz at $M_\infty = 0.7$ - 0.72

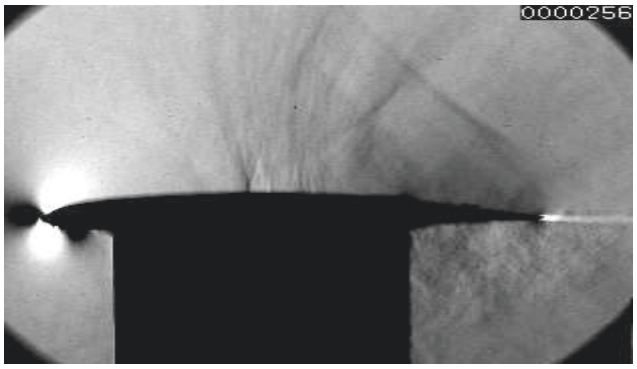

Fig. 6: Schlieren picture at $M_\infty = 0.71$

With an increasing Mach number ($0.7 < M_\infty < 0.72$), but still in the subsonic flow regime, the wave amplitude creates a bell-like shape atop the airfoil (see Fig. 5) whose overall level and the maximal amplitude increases with increasing Mach number. Only at the front quarter of the airfoil the amplitude stays at a constant value. The waves move along the airfoil but are only visible in the midsection of the airfoil (Fig. 6). At a free stream Mach number of 0.72, for the first time, the speed of sound is reached. This was depicted from the pressure coefficient which equals the critical pressure coefficient at a single point on the airfoil. The critical Mach number of 0.72 marks the passage from the subsonic to the intermediate flow regime. If the Mach number is increased further to $0.73 < M_\infty < 0.75$ (Fig. 7) a sudden and significant change in the shape of the amplitude curves occur. The part of constant amplitude in the vicinity of the leading edge now enlarges slightly with increasing Mach number. The inclination of the former bell becomes linear. Unfortunately, the maximal pressure amplitude of $M_\infty = 0.75$ is located downstream of the last pressure sensor of that experiment. Moreover, it is found that the maximal amplitude coincidences with the end of the local supersonic region.

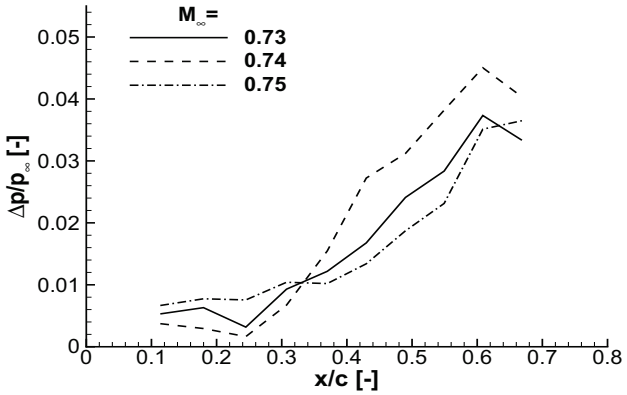

Fig. 7: Pressure amplitude for f = 1 kHz at $M_\infty = 0.73$ - 0.75

In Figure 8 the local pressure coefficient c_p, the critical pressure coefficient c_{pcrit} and the normalized pressure amplitude of the 1 kHz frequency are plotted over the normalized chord length for $M_\infty = 0.74$. At x/c = 0.64 the local pressure coefficient equals the critical pressure coefficient indicating the end of the supersonic region. At the same position the pressure amplitude has its maximum.

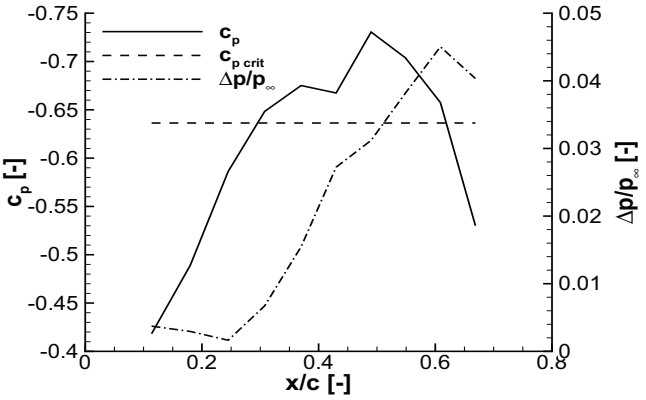

Fig. 8: Pressure coefficient and amplitude for f = 1 kHz over sensor position at $M_\infty = 0.74$

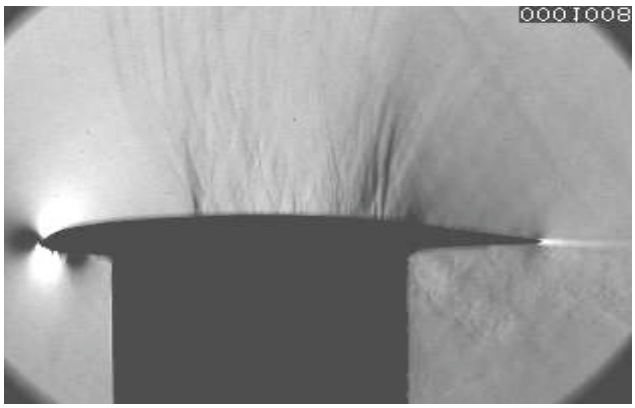

Fig. 9: Schlieren picture at $M_\infty = 0.74$

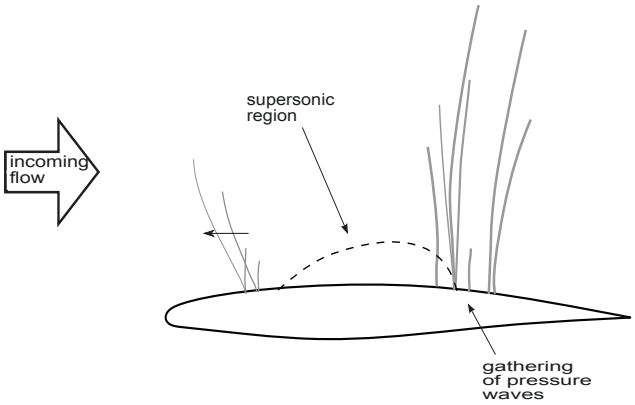

Fig. 10: Sketch of gathering at $M_\infty = 0.74$

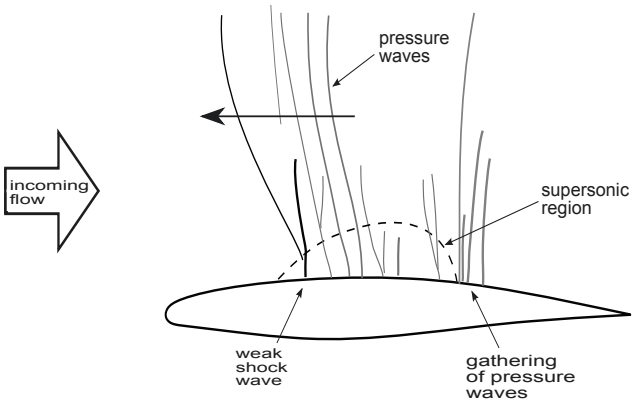

Fig. 11: Sketch of pressure wave movement at $M_\infty = 0.74$

The schlieren movie of the same experiment shows that the waves, moving with the speed of sound, gather at the end of the supersonic region which explains the maximal pressure amplitude at that location (Fig. 10). The pressure waves merge so that a weak shock is formed. Once the shock has gained sufficient strength, it starts crossing the supersonic region. The weak, upstream moving shock induces a local region of subsonic flow behind it so that further pressure waves, coming from the trailing edge, are able to cross the former supersonic region as well (Fig. 9, 11). Although, the weak upstream moving shock influences strongly the local velocity and the local pressure coefficient, the end of the supersonic region fluctuates only within 5% of the chord length.

During the upstream movement, the shock wave first weakens continuously. In the vicinity of the leading edge the weakening process stagnates, so that the pressure amplitude is constant in this part of the airfoil as mentioned above. By the time the shock reaches the point where its amplitude stays constant, the cycle starts again with the gathering of pressure waves at the end of the supersonic region.

Al Shabu [7] could show with a cross-correlation that this weak shock wave moves with a Mach number of around 1.05.

The gathering of the pressure waves at the end of the supersonic region has been observed and been analytically derived with the potential equations by Spee [9] and Voss [2] for two different airfoils. Moreover, this cycle of the wave movement was also observed by Tijdeman [3] in his experiments with an NACA 64A006 airfoil with an oscillating flap at a free stream Mach number of 0.85 and it corresponds to his type C.

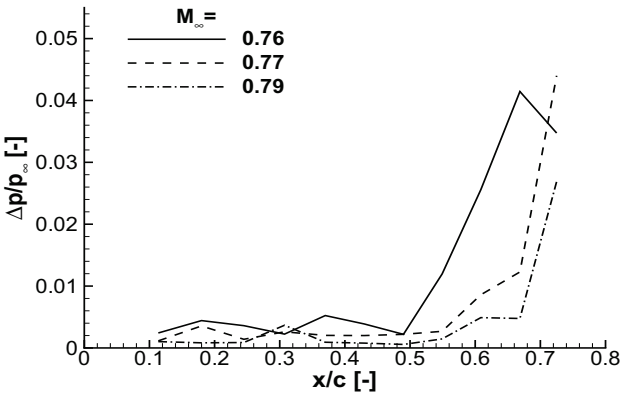

Fig. 12: Pressure amplitude for f = 1 kHz at $M_\infty = 0.76$ - 0.79

The rise of the Mach number to $M_\infty = 0.76$ - 0.79 leads to a stronger increase of the amplitude of the pressure waves. Meanwhile, the maximal amplitude moves clearly downstream (Fig. 12) with the increasing Mach number. This can be explained by the growth of the supersonic region and the formation process of the recompression shock. At $M_\infty = 0.76$ the waves gather still at the downstream end of the supersonic region. At this Mach number, the weak shock waves leave continuously into the supersonic region (see Fig. 1). The flow velocity in the supersonic region stays above the speed of sound while the shock waves are crossing. Therefore, we can observe a continuous gathering process of the waves at the end of the supersonic region. Furthermore, the weakening process of the upstream moving shocks is accelerated so that the shock waves are hardly measurable in the front half of the airfoil.

Fig. 13: Schlieren picture at $M_\infty = 0.77$

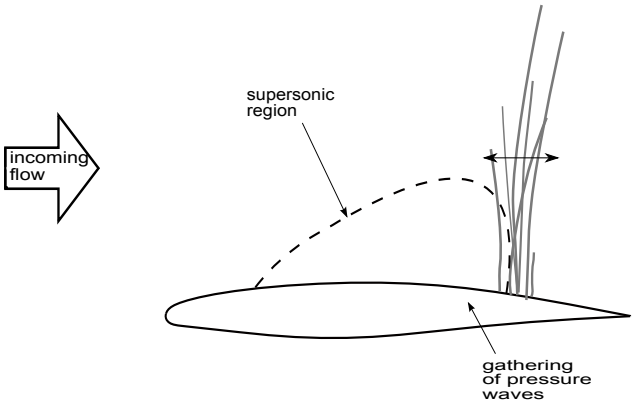

Fig. 14: Sketch of pressure waves at $M_\infty = 0.77$

At $M_\infty = 0.77$ no more shock waves directly leave into the supersonic region (see Figure 13, 14) since the flow velocity is too high. The gathered waves stay at the end of the supersonic region where they slightly oscillate. The amplitude of the pressure fluctuation in the supersonic region decreases to a minimum clearly beyond the amplitude of the waves at the lowest examined Mach number ($M_\infty = 0.63$).
At Mach numbers above $M_\infty \geq 0.78$ the supersonic region ends with a stationary shock. The shock is located downstream of the last sensor but is clearly visible in the schlieren picture (Fig. 15). This marks the beginning of the transonic flow regime. The shock still oscillates and moves downstream with an further increase of the free stream Mach number. The pressure waves move still upstream from the trailing edge towards the stationary shock where they interact with it. Al Shabu and others have observed that the pressure waves travel around the shock along the outer subsonic part. They enter the supersonic part in front of the shock under a large angle to the incoming flow which can be seen in the schlieren image (Fig. 15). If the waves reach the airfoil surface they are to weak to be measured, see Fig. 12.

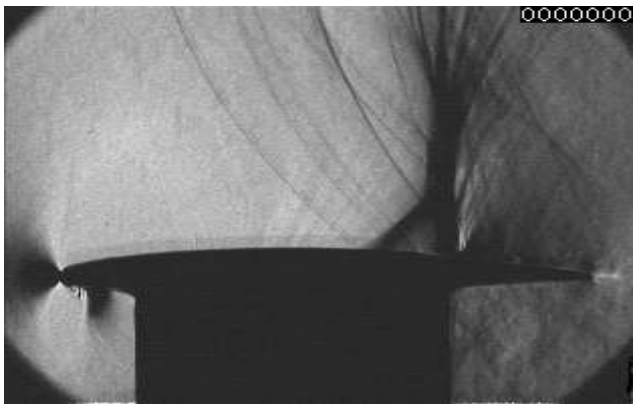

Fig. 15: Schlieren picture at $M_\infty = 0.79$

3.2 Design of Serrated Trailing Edge

In order to reduce the amplitude of the waves a serrated splitter plate was added to the trailing edge. The design of the serration is based on studies of Howe [11, 12], Herr [17] and Dassen et al. [18], all of them dealing again with the noise reduction in flows with free stream Mach numbers less than 0.4.

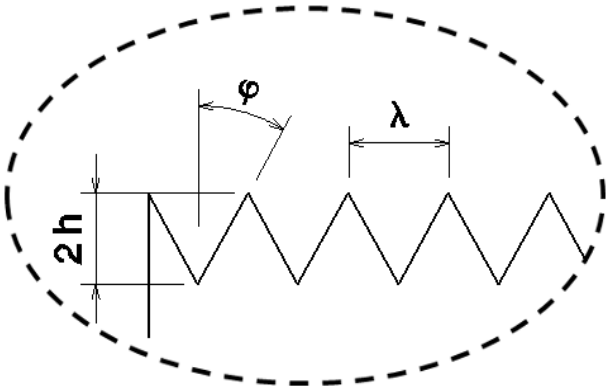

Fig. 16: Sketch of trailing edge serration

Howe [11] suggested in his paper an angle of $\varphi \leq 45°$ in order to reduce the noise generated at a sharp trailing edge of a flat plate airfoil, which is confirmed by Herr [17]. Howe names two different mechanism for the noise reduction with the help of the trailing edge serration. Firstly, the serration reduces the pressure fluctuations in the near-region of the trailing edge. Secondly, it reduces the interaction of the trailing edge with the vortices of the turbulent boundary layer. He found that vortices with a wave-number vector perpendicular to the trailing edge edge have the same dominant, high frequency as the radiated noise. He concluded that a turbulent eddy characterized by the wave-number vector κ in the plane of the airfoil generates significant edge noise only in the neighborhoods of those edge regions where κ is normal to the edge. Recently, papers [19, 20] have been published on experiments of the noise reduction mechanism of serrations saying that a wider angle, in contrast to Howe's theory, outperform the narrower one. Nevertheless, the decision for an angle of $\varphi = 30°$ was chosen before these papers had been published.
Dassen et al. [18] who used a sharp, serrated trailing edge for the noise reduction at $0.12 < M_\infty < 0.22$ of wind turbine blades examined different tooth lengths and orientations. He found the serration to be most effective if the ratio of tooth length to boundary layer thickness is five while the teeth have to be oriented parallel to the flow. The boundary layer thickness of the BAC airfoil at the trailing edge was estimated with the equation for a turbulent boundary layer over a flat plate to $\delta = 1.8$ mm for a Reynolds number of $Re_c = 10^6$, therefore the teeth had to be at least a length of 2h = 9 mm. The boundary layer thickness

was verified by a numerical simulation. In summary, tooth lengths of 2h = 6 mm and 2h = 9 mm have been tested.
The serrated splitter plate has a thickness of 0.1 mm. It was applied at the trailing edge on the pressure side of the airfoil. The transition from the airfoil to the splitter plate was smoothened.

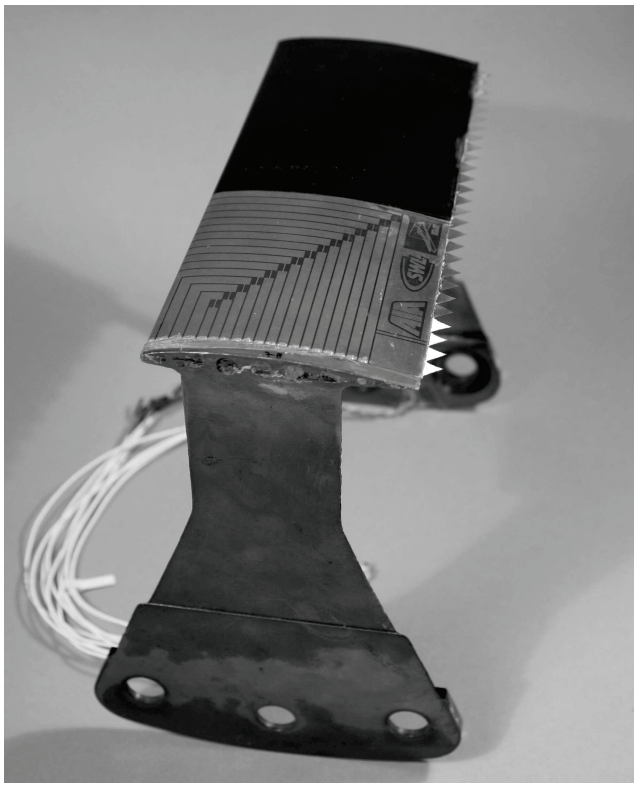

Fig. 17: Wind tunnel model with serrated splitter plate of 6 mm tooth length

3.3 Results of Serrated Trailing Edge

At the very low Mach numbers no clear reduction of the wave amplitude could be observed. Since the pressure waves at these flow velocities are very weak all three amplitude plots level around 0.05 for the 1 kHz frequency (Fig. 18). This holds also for the plots of the 1.5 kHz frequency and the standard deviation which are not shown here. For the sake of brevity only the plots of the 1 kHz frequency are shown in the following.
If the Mach number is increased to 0.68 (Fig. 19) and 0.71 (Fig. 20), the flow is still subsonic, a clear reduction of the wave amplitude is detected for the 9 mm serration. The reduction of the 1 kHz frequency (Fig. 19, 20) and of the standard deviation (not shown) reaches up to 40%. For 1.5 kHz (not shown) the reduction is with up to 50% slightly higher. The 6 mm serration does not indicate any reduction of the wave amplitude what would support the minimal tooth length of 9 mm as stated by Dassen [18].

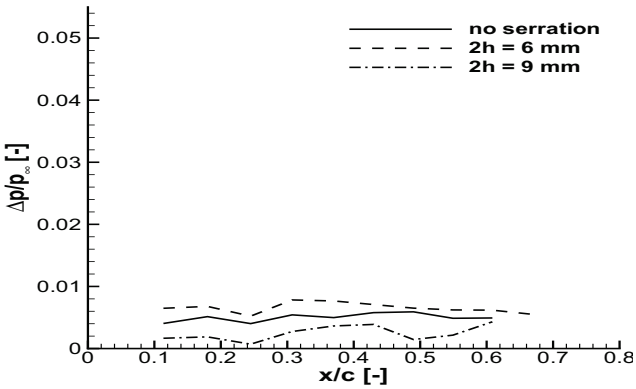

Fig. 18: Pressure amplitude for different serration lengths for f = 1 kHz at $M_\infty = 0.63$

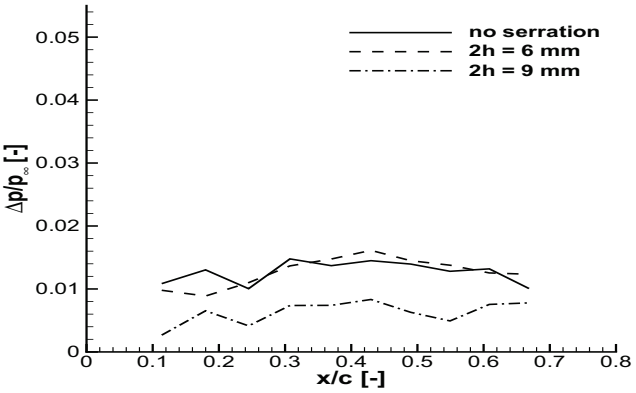

Fig. 19: Pressure amplitude for different serration lengths for f = 1 kHz at $M_\infty = 0.68$

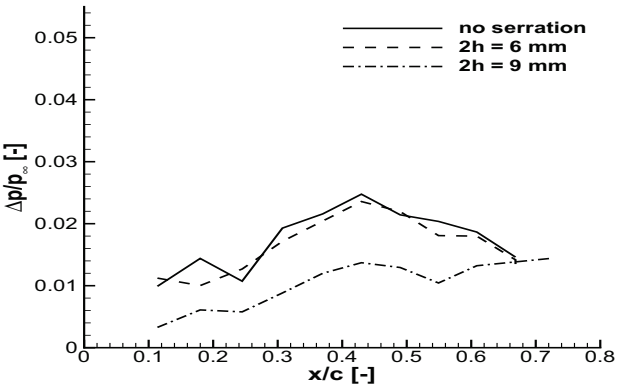

Fig. 20: Pressure amplitude for different serration lengths for f = 1 kHz at $M_\infty = 0.71$

Fig. 21 shows that within the measurement accuracy the serrated splitter plates have no influence on the time-averaged pressure distribution. This holds also for the other examined Mach numbers. Also Oerlemans [13] observed that the trailing edge serrations had no adverse effect on the aerodynamic performance.

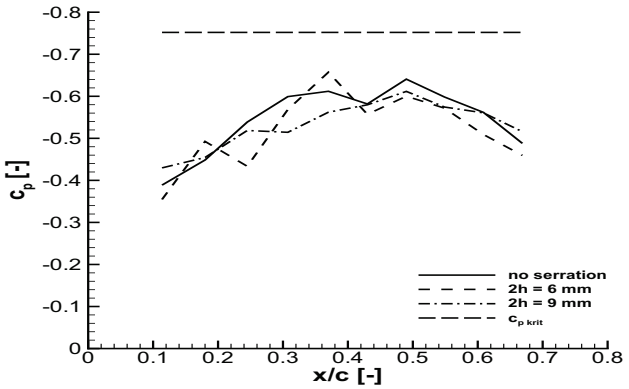

Fig. 21: Pressure coefficient for different serration lengths at $M_\infty = 0.71$

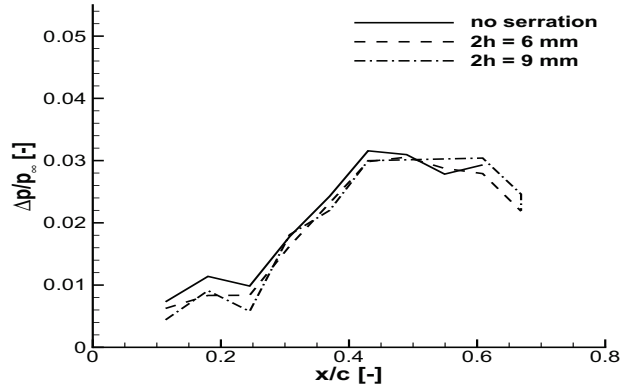

Fig. 22: Pressure amplitude for different serration lengths for f = 1 kHz at $M_\infty = 0.72$

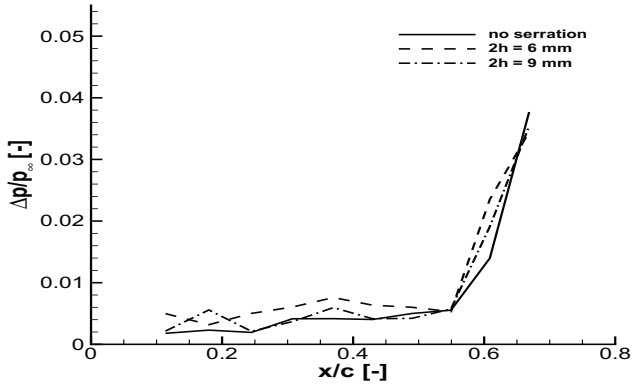

Fig. 23: Pressure amplitude for different serration lengths for f = 1 kHz at $M_\infty = 0.76$

A further increase of the Mach number leads to the intermediate regime where no reduction of the wave amplitude could be detected. At the critical Mach number of 0.72, where the waves still move as a wave package with a leading shock over the airfoil and where the flow velocity reaches the speed of sound for the first time, no reduction was measurable anymore (Fig. 22). At the higher Mach numbers where the waves gather at the end of the supersonic region also no reduction was found (Fig. 23). In this Mach number regime, the intermediate flow regime, it appears that steepening and gathering effects of the waves are so dominant that they overcome the reduction of the pressure amplitude at the trailing edge.
At Mach numbers above $M_\infty = 0.78$ with a stationary shock no statement can be given on the wave reduction since no pressure taps could be placed between the shock and the trailing edge.

4 CONCLUSION

The current investigation shows the strong dependence of the propagation behavior of upstream moving pressure waves on the free stream Mach number. Three different flow regimes have been defined, the pure subsonic with weak pressure waves moving along the complete airfoil; the intermediate one with no stationary shock but with weak shock waves crossing the supersonic regime; and the transonic regime with a stationary shock where the pressure waves move up to the shock and only a few move around the shock.
In the second part, the influence of a serrated splitter plate at the trailing edge on the pressure waves was examined in dependence of the free stream Mach number. A clear reduction of the pressure wave amplitude could be achieved in the subsonic Mach number range ($0.68 < M_\infty < 0.71$) but no reduction for the waves could be achieved at Mach numbers higher than the critical Mach number ($M_{crit} = 0.72$) for which locally velocities higher than the speed of sound are reached. It could be shown further that a tooth length of five times the boundary layer thickness, as stated by Dassen [18], is sufficient to reduce the wave amplitude in the subsonic flow regime.
For more details, investigations should be made on serrations with different angles and an even longer tooth length. Also additional sensors need to be placed in the vicinity of the trailing edge in order to measure the pressure wave amplitude between the stationary shock and the trailing edge.

Acknowledgments

This research was funded by the German Research Foundation within the project “Numerische und experimentelle Untersuchung zur Abschwaechung stromauf laufender Druckwellen bei transsonischer Profilumstroemung” (DFG OL 107/22) which is gratefully acknowledged.

LITERATURE

[1] Lee, B. H. K., *Self-sustained shock oscillations on airfoils at transonic speeds*, Progress in Aerospace Sciences, 2001, Vol. 37, No. 2, pp. 147-196.

[2] Voss, R., *Ueber die Ausbreitung akustischer Stoerungen in transsonischen Stroemungsfeldern von Tragfluegeln*, DFVLR Forschungsbericht, Institut für Aeroelastik, Göttingen, 1988.

[3] Tijdeman, H., *Investigation of the transonic flow around oscillating airfoils*, PhD thesis, Technische Hogeschool Delft, 1977.

[4] Hermes, V. and Klioutchnikov, I. and Alshabu, A. and Olivier, H., *Investigation of unsteady transonic airfoil flow*, AIAA 2008-627, 46th AIAA Aerospace Sciences Meeting and Exhibit, Reno, 2008.

[5] Klioutchnikov, I. and Olivier, H., *A numerical study of pressure/shock waves interactions in transonic airfoil flow using optimized WENO schemes*, AIAA 2010-924, 48th AIAA Aerospace Sciences Meeting, Orlando, 2010.

[6] Hermes, V. and Klioutchnikov, I. and Olivier, H., *Numerical investigation of unsteady wave phenomena for transonic airfoil flow*, Aerospace Science and Technology, Vol. 25, No. 1, pp. 224-233, 2013. DOI:10.1016/j.ast.2012.01.009

[7] Al Shabu, A., *Instationaere Wellenphaenomene bei der Profilumstroemung im Transschall*, PhD thesis, RWTH Aachen University, 2010.

[8] Ballmann, J. and Boucke, A. and Chen, B. and Reimer, L. and Behr, M. and more, *Aero-Structural Wind Tunnel Experiments with Elastic Wing Models at High Reynolds Numbers (HIRENASD - ASDMAD)*, AIAA2011-882, 49th AIAA Aerospace Sciences Meeting including the New Horizons Forum and Aerospace, Orlando, Florida, 2011.

[9] Spee, B., *Wave propagation in transonic flow past two-dimensional aerofoils*, National Lucht- en Riumtevaartlaboratorium, NLR-TN T.123, 1966.

[10] Nieuwland, G. Y., *The computation by Lighthill's method of transonic potential flow around a family of quasi-elliptical aerofoils*, NLR-TR T.83, 1964.

[11] Howe, M. S., *Noise produced by a sawtooth trailing edge*, The Journal of the Acoustical Society of America, 1991, pp. 482 - 487.

[12] Howe, M. S., *Aerodynamic noise of a serrated trailing edge*, Journal of Fluids and Structures, No. 5, 1991, pp. 33 - 45.

[13] Oerlemans, S. and Fisher, M. and Maeder, T. and Koegler, K., *Reduction of Wind Turbine Noise Using Optimized Airfoils and Trailing-Edge Serrations*, AIAA Journal, Vol. 47, No. 6, pp. 1470-1481, 2009.
doi: 10.2514/1.3888

[14] Jones, L. E. and Sandberg, R. D., *Acoustic and hydrodynamic analysis of the flow around an aerofoil with trailing edge serrations*, Journal of Fluid Mechanics, Vol. 706, 2012, pp. 295–322.

[15] Zechner, M., *Transsonische Profilumstroemungen im Stossrohr- Transschallkanal*, PhD thesis, RWTH Aachen University, 2002.

[16] Alshabu, A. and Olivier, H., *Unsteady wave phenomena on a supercritical airfoil*, AIAA Journal, Vol. 46, No. 8, 2008, pp. 2066-2073.

[17] Herr, M., "On the Design of Silent Trailing-Edges", *New Results in Numerical and Experimental Fluid Mechanics*, Vol. 6, No. 96, 2007, pp. 430-437.
chapter doi: 10.1007/978 − 3 − 540 − 74460 − 3_53

[18] Dassen, T. and Parchen, R. and Bruggeman, J. and Hagg, F., *Results of wind tunnel study on the reduction of airfoil self-noise by the application of serrated blade trailing edges*, NLR TP 96350, 1996.

[19] Chong, T. P. and Joseph, P. and Gruber, M., "An Experimental Study of Airfoil Instability Noise with Trailing Edge Serrations", *16th AIAA/CEAS Aeroacoustic Conference (31th AIAA Aeroacoustic Conference)*, Stockholm, Sweden, AIAA 2010-3723.
chapter doi: 10.2514/6.2010-3723

[20] Moreau, D. J. and Brooks, L. A. and Doolan, C. J., "On the Noise Reduction Mechanism of a Flat Plate Serrated Trailing Edge at Low-to-Moderate Reynolds Number", *18th AIAA/CEAS Aeroacoustics Conference (33rd AIAA Aeroacoustics Conference)*, 4-6 June 2012, Colorado Springs, CO, AIAA 2012-2186.
chapter doi: 10.2514/6.2012-2186